Poly(indole-6-carboxylic acid)/Carbon Composite as the Matrix for the Immobilization of the Phenanthroline Metal Complexes, and the Use of the Composites as Electrocatalyst for Oxygen Reduction Reaction

Xilin Wang[1], Min Wang[2], Xiuping Ju[3], Yan Zhang[1], Jinsheng Zhao[1,*], Junhong Zhang[1,*]

[1]Shandong Key Laboratory of Chemical Energy Storage and Novel Cell Technology, Liaocheng University, Liaocheng, 252059, P. R. China
[2]Liaocheng People's Hospital, Liaocheng 252000, P.R. China
[3]Dongchang college, Liaocheng University
[*]E-mail: j.s.zhao@163.com, zhangjunhong@lcu.edu.cn

Two new none-precious metal electro-catalyst for the reduction of oxygen (ORR) were prepared by a facile method, which is characterized by the sequential procedure including oxidation polymerization, chemical coupling and ion complexation reactions etc. The carbon supported poly(indole-6-carboxylic acid) composite (PIn/C) was obtained by the in-situ polymerization method, which was linked with 5-amine-1,10-phenanthroline to form the PInPhen/C composite, and the final CuPInPhen/C or FePInPhen/C catalysts were obtained by the complexation reaction of PInPhen/C with Cu (II) or Fe (II) ions. The morphologies and chemical compositions of the catalysts were studied by scanning electron microscopy (SEM) and X-ray photoelectron spectroscopy (XPS) method. The electrochemical behaviour of the catalysts were characterized using techniques such as cyclic voltammetry (CV), rotating disk electrode (RDE), rotating ring-disk electrode (RRDE) and electrochemical impedance spectroscopy (EIS). The data of the results suggested that both of the composite catalysts underwent a predominant four-electron pathway for the reduction of oxygen, with the CuPInPhen/C catalyst exhibited a better ORR activity and stability than that of the FePInPhen/C catalysts.

1. INTRODUCTION

Fuel cells have been considered as one of the most promising energy conversion devices during the last decades, due to its high power density and conversion efficiency, quick start-up and environmental-friendly nature [1-2]. However, many problems hindered its commercialization which are high costs and difficult preparation of electrocatalysts used in cathode. For a long time, platinum

(Pt) has been considered to be the best catalyst for ORR, although it remains impractical due to the high cost and tend to instability during the ORR process [3-4]. It is worth noting that the cost of cathode materials accounting for almost half of total cost of fuel cells due to the use of precious metal Pt. In order to reduce the costs of catalysts, the Pt-based metallic electrocatalysts, such as Fe [5], Co [6], Ni [7], Cu [8], V [9], and Cr [10]alloying with Pt had been prepared for ORR. Besides, the development of non-precious metal even metal-free oxygen reduction reaction catalysts replacing Pt plays a critical role in marketization of fuel cells in the aspects of costs and the fuel cell performance [11-12]. At present, it is essential to find new, available and better electrocatalysts, especially none-noble oxygen reduction (ORR) for the devices.

To reduce or replace Pt-based catalysts, conjugation polymers are widely used in the preparation of oxygen reduction catalysts. It can be used as supporting materials, the precursors of doped nitrogen atoms [13], and even the polymer itself can be used as ORR catalysts. Taking advantage of their satisfactory stability, accessible conductivity, high specific surface area, as well as the facile preparation, conjugated polymers such as polythiophene (PTh) and polyaniline (PAn) have been frequently employed in the preparation of ORR catalysts [14-16]. Besides, some carbon materials including carbon black, graphene and carbon nanotubes (CNTs) were often used as carrier of catalysts because of the low prices, and the ability to increase the surface area of the surface covered polymer. Carbon blacks are the least expensive and most suitable carbon material which can enhance the conductivity of catalyst greatly in the application of fuel cell [17-18]. And also, the composites of the conductive polymers and the carbon materials have already been extensively studied and shown ideal results in the field of ORR due to the nice combination of the properties and easy preparation [19]. Some of the copper (II) complexes with 1,10-phenanthroline (phen), 5-chloro-1,10-phenanthroline etc., were prepared by Anson and coworkers [20-22], which could lead to a mixture of the $[CuL]^{2+}$ or $[CuL_2]^{2+}$ complexes and showed quite impressive ORR performance.

Based on the above discussion, the M-phen complexes decorated poly(indole-6-carboxylic acid)(CuPInPhen/C, FePInPhen/C) has been synthesized via a chemical process, which has the following merits: (a) the PIn/C composite is facilely prepared by a oxidative-polymerization method; (b) the 5-Amine-1,10-phenanthroline molecular was bonded with the PIn/C composite through the chemical bonding of amino group and carboxyl group and the formation of PInPhen/C composite; (c) two none-noble ORR catalysts were obtained by the complexation of the Cu (II) or Fe (II) ions with the PInPhen/C composite. The electrochemical behavior of the ORR catalysts was studied by using cyclic voltammetry (CV), rotating disk electrode (RDE) and rotating ring disk electrode(RRDE) techniques in 0.1 M phosphate buffer. The prepared none-noble ORR catalysts present preferable ORR performance in phosphate buffer solutions, which is suitable for cathode catalyst for fuel cells, especially for microbial fuel cells.

2. EXPERIMENTAL

2.1. Materials

N-(3-dimethylaminopropyl)-N'-ethylcarbodiimide hydrochloride (EDAC) (AR, 98.5%), N-hydroxysulfosuccinimide sodium salt (NHS) (AR, 98%), C_2H_5OH (AR, 95%), $HClO_4$ (AR, 70.0-

72.0%), $NaH_2PO_4 \cdot 2H_2O$ (AR), $Na_2HPO_4 \cdot 12H_2O$ (AR), $FeSO_4$ (AR), $CuSO_4$ (AR), $K_3[Fe(CN)_6]$ (AR), $K_4[Fe(CN)_6] \cdot 6H_2O$ (AR), KCl (AR), $FeCl_3 \cdot 6H_2O$, KOH (AR) were all obtained from Aladdin Reagent and be used directly. Indole-6-carboxylic acid (AR) and 5-Amine-1,10-phenanthroline (AR) were received from J & K. The catalyst suspensions which are to be used in the working electrode are prepared in the following way: 1.6 mg of the composite samples, 177 µL of isopropanol (Aladdin, AR), and 3 µL of nafion solution (Dupont, 5 wt%) were mixed with 570 µL of ultra-pure water and the mixture were furthur ultrasonic mixed in an ultrasonic bath (KQ-600KDE, 600 W) for 1 hour [23]. After that, the suspension was quantitatively transfered on the glassy carbon electrode and be used after 15 min for the natural evaporation of water. Ultra-pure nitrogen or oxygen were bubbled into the testing solutions for at least 30 min to get a oxygen-free or oxygen-saturated atmosphere.

2.2. Preparation of electrocatalyst

The carbon supported polyindole-6-carboxylic acid precursor was prepared by a modified method as follows: 1 g of Vulcan XC-72 carbon (Cabot, BET surface area of 235 $m^2 g^{-1}$, denoted as C) was suspended in 50 mL of ethanol and resulting slurry was stirred under constant speed for 30 min at room temperature. And then, the slurry was ultrosonicated for 1 h, after which, 1 g (6.2 mmol) of indole-6-carboxylic acid and 50 mL of $FeCl_3 \cdot 6H_2O$ (12.4 mmol) aqueous solution were added into the slurry. The resulting slurry was stirred overnight at dark conditions, and the carbon supported polyindole-6-carboxylic acid slurry (PIn/C) was formed. The resulting black precipitate was separated by centrifugation at 8000 rpm, washed with ethanol for several times and then dried overnight at 60 °C in a vacuum oven.

In order to prepare the PInPhen/C composite, the obtained PIn/C composite was dispersed in 50 mL of 0.2 M phosphate buffer (pH 5.7) in an ice bath. After which, 3.26 g (21 mmol) of EDAC was added to the slurry and incubated for 0.5 h, and then 0.80 g (7 mmol) of NHS was put into the reaction slurry. After stirring for 2 h, 0.30 g (1.54 mmol) of 5-Amine-1,10-phenanthroline of ethanol solution (50 mL) was put into the slurry dropwise along with vigorously stirring for further 24 hours. Finally, the black precipitate was separated by centrifugation at 8000 rpm, washed with ethanol and ultrapure water for several times, and then dried overnight at 60 °C in a vacuum oven.
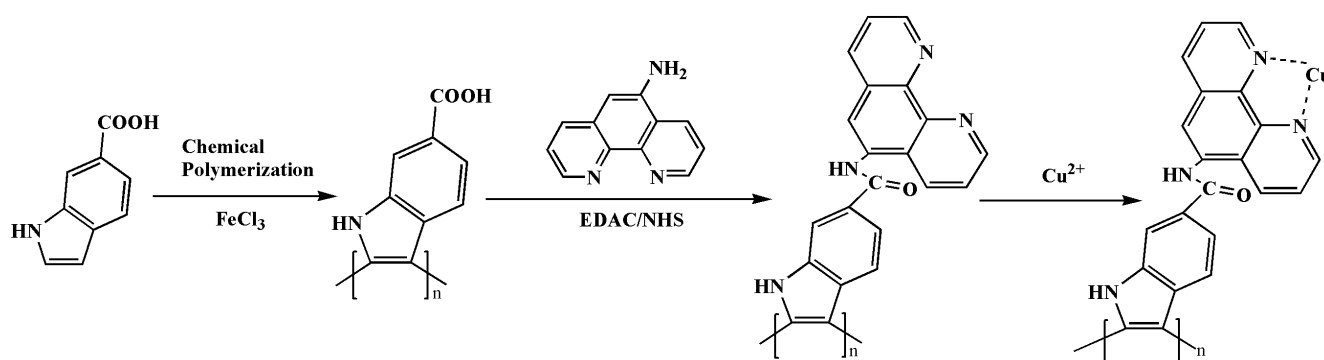
Scheme 1. Schematic diagram of synthetic process of CuPInPhen.

The fabrication of the CuPInPhen/C catalyst was shown as below: 0.6 g of $CuSO_4$ was added into the PInPhen/C slurry with stirring for 2 hours, then the prepared CuPInPhen/C composite was washed for several times and dried in a vacuum oven at 60 °C for 24 h. The technical route for the preparation of the CuPInPhen/C catalyst was shown in Scheme 1. The preparation procedure of the FePInPhen/C catalyst is the same as the CuPInPhen/C catalyst except for the incorporated metal ions. For FePInPhen/C, Fe (II) was used as the incorporated metal ions.

2.3. Electrode preparation and electrochemical measurements

Cyclic voltammetry (CV) studies were made on a Autolab potentiostat/galvanostat (PGSTAT302N) station, equipped with a standard three-electrode electrochemical cell and a gas flow system. The RDE and RRDE voltagrammetry experiments were performed by linear sweep voltagrammetry (LSV) on an electrode rotator (AFMSRCE, Pine) and recorded by a potentiostat/galvanostat (autolab PGSTAT 302N). The working electrode employed in the CV and the RDE studies was a glass carbon electrode with a diameter of 5.0 mm. And, the working electrode in the RRDE experiments was a pine model AFE7R9GCPT electrode with a 5.61 mm diameter glassy carbon disk and a Pt ring with an inner diameter of 6.25 mm and an outer diameter of 7.92 mm. A Platinum foil and Ag/AgCl/sat. KCl electrode were served as the counter and reference electrode, respectively.

For CV, RDE and RRDE measurements, the aqueous solutions of 0.1 M phosphate buffer solution (PBS, pH=7.0), $HClO_4$ or KOH were employed as the test medium. N_2 or O_2 was utilized to bubble the medium to get a oxygen-free or oxygen-saturated mediums, respectively.

The working electrodes were finely polished with alumina suspension (0.3 μm) and rinsed thoroughly with ethanol and water in an ultrasonic bath to remove any alumina residues to create a mirror finish. Then, 8.0 μL of the catalyst slurry was quantitatively transferred to the working electrode by a micropipette, and be left to air dry for further studies and characterization. Prior to each measurement, high-purity N_2 or O_2 was bubbled into the electrolytic cell for about 30 minutes and the gas was made to flushed over the solution throughout the studies. Furthermore, twenty cycles of CV performance between -0.8 and 0.5 V vs. Ag/AgCl/sat. KCl electrode at a scan rate of 100 mV s^{-1} were conducted to activate the working electrode.

2.4. Physical characterization

The micromorphology of the as prepared composite were measured using scanning electron microscope (SEM, SU 8020) under an accelerating voltage of 1.0 kV. The samples used for SEM were prepared by quantitatively dripping catalyst slurry on the ITO coated glass. The surface element characterization of the synthesized catalysts were conducted by X-ray photoelectron spectroscopy (XPS, ESCALAB 250Xi) using a monochromatic Al K_α (1486.6 eV) radiation. All the electron binding energies of XPS were referenced to C 1s of carbon at 284.6 eV and these experiments were carried out under ultra-high vacuum. The XPS curves were fitted with a mixed Gaussian/Lorentzian

fitting using the XPS peak fit 4.1 software, and a baseline fitting was conducted with a polynomial multi-point fitting carried out with the same software.

3. RESULTS AND DISCUSSION

3.1 Structure and composition characterization of catalysts

3.1.1 Morphology analysis by SEM

Morphological structures of the prepared catalysts was studied by SEM, and the results displayed different surface morphologies among the carbon material and the as prepared CuPInPhen/C or FePInPhen/C catalysts. As seen in Fig. 1a, the carbon black shows an amorphous structure consisting of many small particles with the sizes of 35-60 nm. Different with that of the Vulcan XC-72 carbon, both of the catalysts show a ooral like porous structure, with the particle sizes of 50-70 nm for CuPInPhen/C catalyst (Fig. 1b), and the particle size of FePInPhen/C ranges between 50-80 nm (Fig. 1c). Furthermore, the particles of the prepared catalysts CuPInPhen/C and FePInPhen/C are interconnected with each other to form a porous net-shape structure with different particle sizes as shown in Fig. 1. Compared with the Vulcan XC-72 carbon, the increased particle sizes of the catalysts might be an indication of the formation of the CuPInPhen or FePInPhen layer on the surface of the carbon particles. We can also observed that the morphology of CuPInPhen/C is much similar with that of the FePInPhen/C catalyst, which indicates that the complexation of different metal ions has no obvious impact on the morphological structure of the catalysts [24]. Moreover, oxygen can freely access through the regular porous framework during the oxygen reduction reaction, which may accelerate the electrocatalytic process and lead to a satisfactory ORR performance.
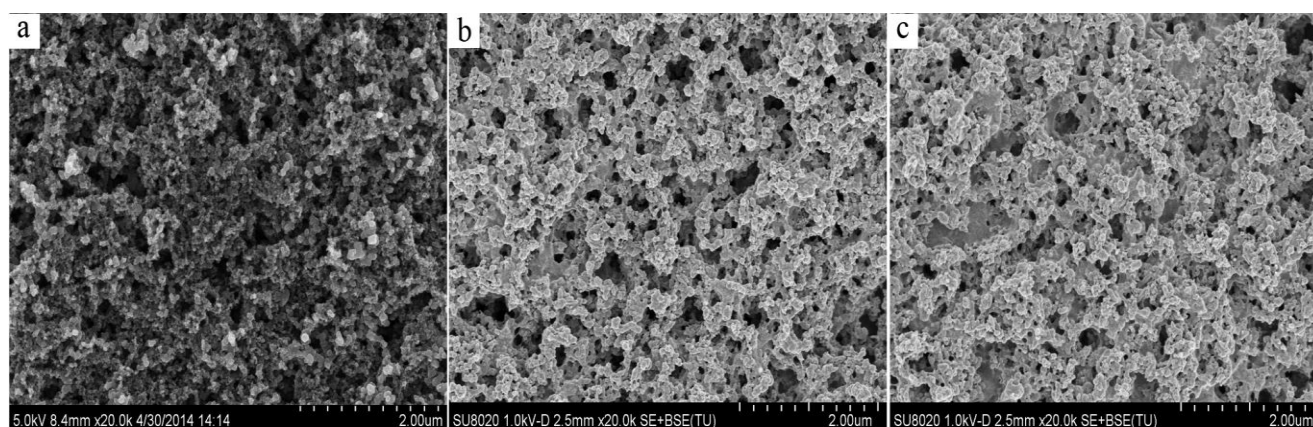

Figure 1. SEM images of (a) Vulcan XC-72/C (b) CuPInPhen/C (c) FePInPhen/C catalysts.

3.1.2 Chemical composition analysis by XPS

The chemical compositions of the as-prepared CuPInPhen/C and FePInPhen/C composites were examined by XPS measurements (Fig.2). As expected, from the survey scans of the XPS spectra

of the CuPInPhen/C (Fig.2 a_1) and the FePInPhen/C (Fig.2 a_2) catalysts, which contain peaks for C, N, Cu, and, C, N, Fe, respectively. As shown in Fig. 2b_1, the N 1s spectra of CuPInPhen/C is dominated by a main peak at 400.5 eV, which can be assigned to pyrrolic N, arising from the polymerization of indole-6-carboxylic acid on the carbon surface. A pronounced N 1s signal peak locates at 399.9 eV can be ascribed to the amine & amide groups formed between the reaction of carboxylic acid groups in poly(indole-6-carboxylic acid) and the amine groups in 5-Amine-1,10-phenanthroline molecules. The immobilization of the 5-Amine-1,10-phenanthroline on the side chains of the poly(indole-6-carboxylic acid) can also be indicated by the presence of the N 1s signal peak locates at 399.4 eV, which can be assigned to the pyridinic N [25-26]. The function of these types of nitrogen towards transition metal-based nitrogen-containing ORR catalysts has been discussed in the literatures [27-28]. As shown in Fig. 2c_1, the Cu 2p peaks were distinctly displayed to further confirmed the successful formation of CuPInPhen/C. The figure shows two pairs of doublets along with the satellite structure which indicated that dissociative Cu (II) ions occur on the surface of the CuPInPhen/C sample. The presence of Cu (II) ions was also affirmed by the typical dissociative Cu $2p_{3/2}$ values of 935.8 eV and Cu $2p_{1/2}$ values of 955.6 eV.
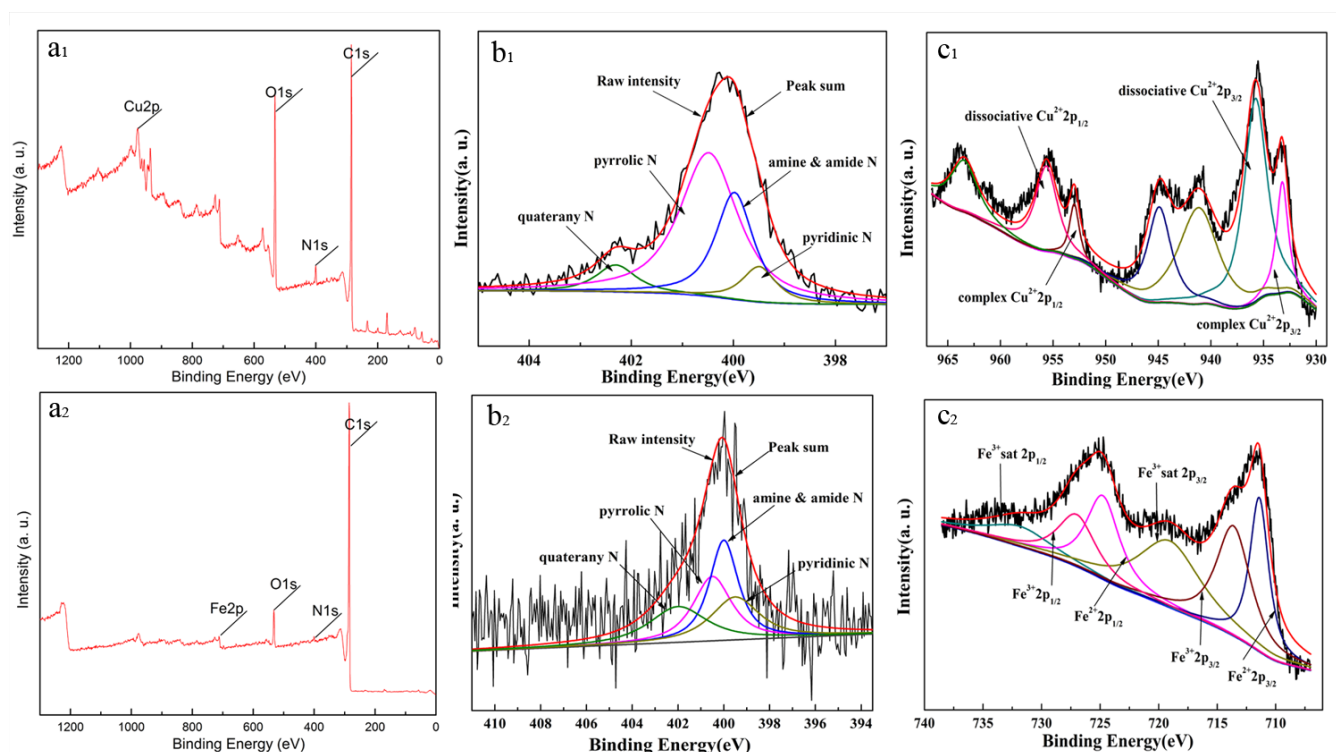

Figure 2. The XPS survey of CuPInPhen/C (a_1) and FePInPhen/C (a_2), N 1s of CuPInPhen/C (b_1) and FePInPhen/C (b_2), the Cu 2p (c_1) of the CuPInPhen/C catalyst and the Fe 2p (c_2) of the FePInPhen/C catalyst.

The positions of the Cu $2p_{3/2}$ and $2p_{1/2}$ core level peaks shifted down to around 933.2 eV and 953.0 eV indicating the copper ions have been successfully incorporated into the composite [29]. Furthermore, the peaks located at 941.2 eV and 944.9 eV can be attributed to the copper oxide which was formed by oxidation of copper ions during the reaction. In order to understand the surface

chemical composition of catalysts better, the N 1s peaks (Fig. 2b$_2$) of the FePInPhen/C were measured and the results similarly illustrated the successful formation of FePInPhen/C. As shown in Fig. 2c$_2$, the Fe 2p peaks were tested and the Fe 2p$_{3/2}$ and 2p$_{1/2}$ peaks located at 711.4 eV and 724.8 eV can be attributable to the Fe^{2+} for FePInPhen/C. Besides, we observed characteristic peaks for Fe^{3+} 2p$_{3/2}$ and 2p$_{l/2}$ at 713.6 eV and 727.0 eV, which signed the appearance of the Fe^{3+} satellite peaks. The presence of the Fe^{3+} largely due to the oxidation of Fe^{2+} during the reaction, because of the instability of dissociative Fe^{2+} [30]. We further demonstrated the occurrence of Fe^{3+} by Fe^{3+} 2p$_{3/2}$ and 2p$_{l/2}$ peaks with the values of 719.0 eV and 731.8 eV [31] which had been displayed in Fig. 2c$_2$. To sum up, based on the XPS analyses, two novel none nobel oxygen reduction catalysts have been successfully synthesized on carbon and conductive polymer materials.

3.2 Electrochemical measurements
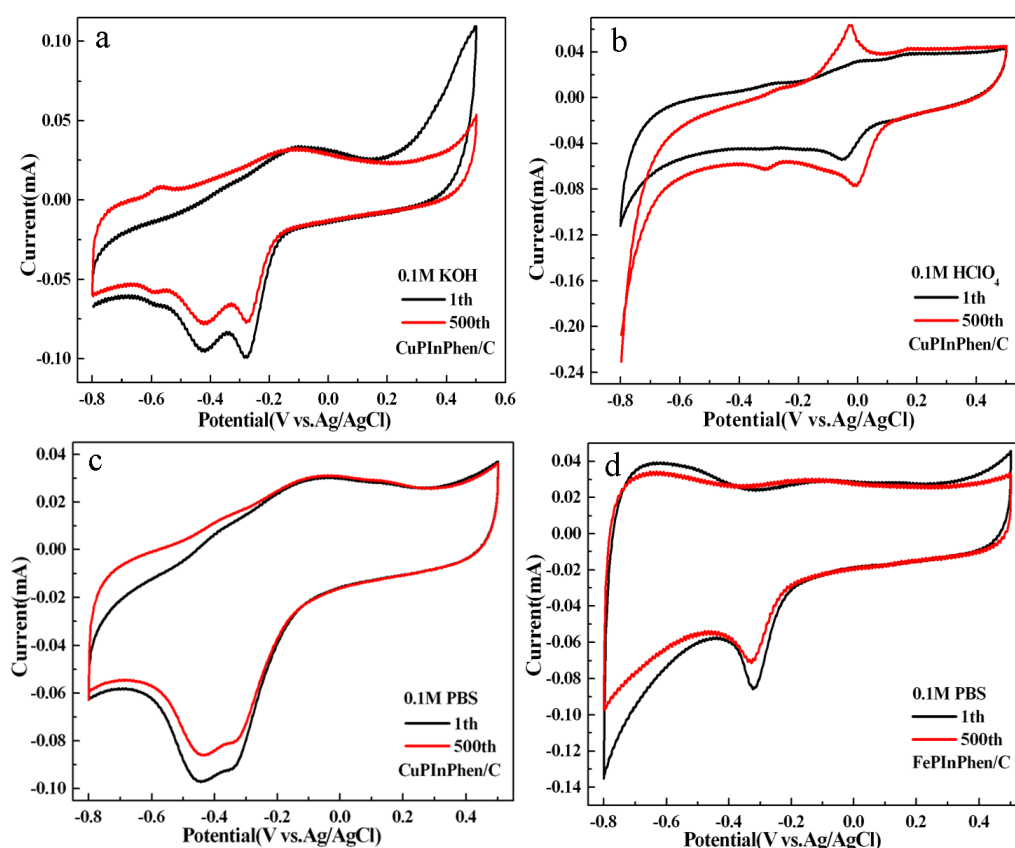
3.2.1 CV measurments of the catalysts

Figure 3. (a), (b), (c) CV of CuPInPhen/C catalyst in N$_2$-saturated 0.1 M KOH, HClO$_4$, PBS (pH=7) aqueous solution, respectively; Scan rate:100 mV s^{-1}. (d) CV of FePInPhen/C recorded in N$_2$-saturated 0.1 M PBS (pH=7) aqueous solution. Scan rate:100 mV s^{-1}

The CV curves of the CuPInPhen/C composite was tested in N$_2$-saturated 0.1 M HClO$_4$, KOH and PBS solution with the subjective for screening the most preferred testing medium (Fig.3a, 3b, 3c). The PBS buffer was finally selected as the best electrolyte for the further study of catalysts owing to

the best stability exhibited as the minimal loss in peak currents after 500 cycles in the PBS buffer solution. And the stability of the FePInPhen/C catalyst was also studied by the continuous CV tests up to 500 cycles as depicted in Fig.3d. It is apparent that the reduction in peak currents was 11.5% and 16.8%, respectively, for the CuPInPhen/C and FePInPhen/C composites. The data showed that the stability of the CuPInPhen/C composite is somewhat higher than that of the FePInPhen/C composite, and might be a more preferable ORR catalyst.

In order to further confirm the ORR performance of the catalyst, the CV of the catalysts were also conducted in O_2-saturated 0.1 M PBS buffer. And, the changes in the ORR peak currents measured between N_2-saturated and O_2-saturated solutions are the most obvious basis for ORR judgment. The greater change in maximum peak current often suggested a better ORR performance. As displayed in Fig. 4a and 4b, the ORR peak potentials of CuPInPhen/C and FePInPhen/C maintain a constant position, while the peak current greatly increased in the O_2-saturated PBS solution than that of the N_2-saturated solution, which confirmed the ORR property of the catalyst. In addition, it is further found in Fig. 4c that the CuPInPhen/C catalyst presents a higher cathodic current density and a more positive peak potential than that of FePInPhen/C in O_2-saturated PBS solution, indicating that the CuPInPhen/C composite might possess a stronger ORR catalytic performance than that of the FePInPhen/C composite.
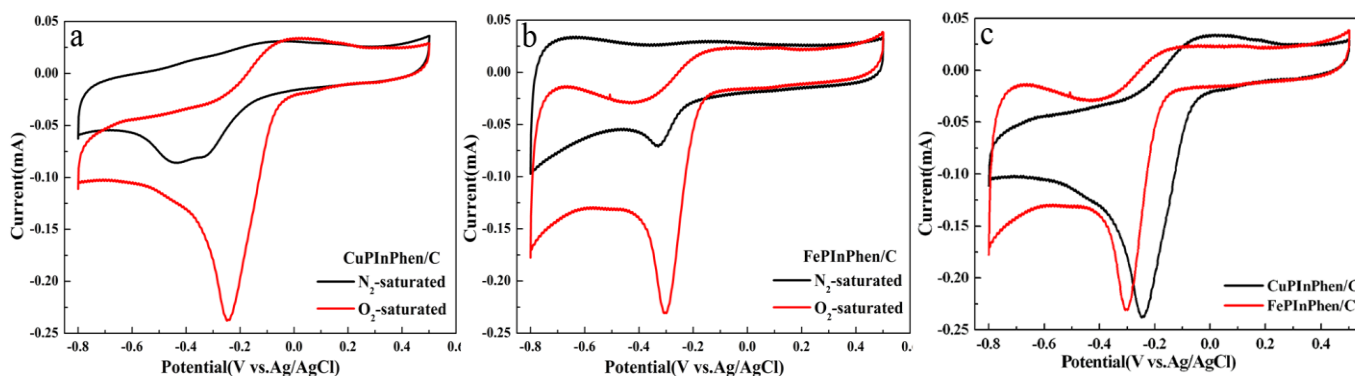

Figure 4. (a), (b) CV of CuPInPhen/C and FePInPhen/C in O_2-saturated and N_2-saturated 0.1 M PBS (pH=7) aqueous solution between -0.8 and 0.5 V. Scan rate:100 mV s^{-1}. (c) CV of CuPInPhen/C and FePInPhen/C recorded in O_2-saturated 0.1 M PBS (pH=7) aqueous solution. Scan rate:100 mV s^{-1}

3.2.2 RDE measurement of the catalyst

The ORR performance of the composites were further investigated using RDE technique in O_2-saturated PBS buffer at a rotation rate of 1600 rpm, and the data was shown in Fig. 5. The polarization curve of CuPInPhen/C exhibits two distinctly different potential regions including a mixed kinetic-diffusion control region between -0.6 V and -0.081 V and a diffusion-limiting current region under -0.6 V. A obvious shift of 41 mV was observed in the onset potential for CuPInPhen/C compared to FePInPhen/C, indicating a enhancement of the ORR activity. In addition, it is also observed that the CuPInPhen/C catalyst has a higher current density value of 4.58 mA cm^{-2} than that of the FePInPhen/C

catalyst (4.13 mA cm^{-2}) at -0.55 V, as listed in Table 1. These results above suggesting that the CuPInPhen/C had a better ORR activity than that of the FePInPhen/C catalyst.
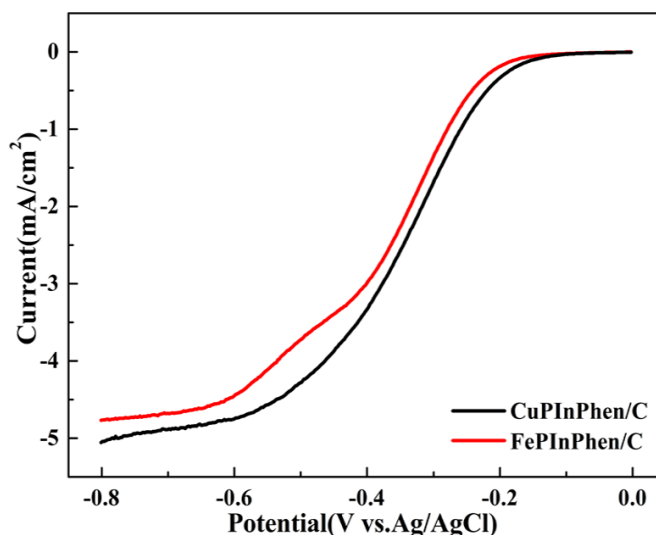

Figure 5. Polarization curves for ORR in O$_2$-saturated 0.1 M PBS (pH=7) aqueous solution. The potential scan rate was 10 mV s^{-1}, and the electrode rotation speed was 1600 rpm.

To elucidate the electron transfer kinetics mechanisms of these catalysts, RDE measurement were used to obtain linear sweep voltammetry curves which were tested between -0.1 and -0.8 V in O$_2$-saturated PBS buffer. As shown in Fig. 6, the curves measured in different rotation rates exhibit a similar trends and a constant initial oxygen reduction potential value. Furthermore, the current densities continually increased with the rising rotation speeds indicating that the higher the electrode rotation speed, the more oxygen it is transferred through the solution bulk to the electrode [32].

The kinetic analysis was also conducted by calculating electron transfer number n during ORR with the Koutecky-Levich (K-L) equation as shown below [33]:

$$\frac{1}{i} = \frac{1}{i_k} + \frac{1}{B\omega^{1/2}} \qquad (1)$$

$$B = \frac{0.62nFC_0D_0^{2/3}}{\eta^{1/6}} \qquad (2)$$

in which i is the mixed kinetic-diffusion current which was measured from polarization curves, i_k is the kinetic current, B is the Levich constant, ω is the angular velocity of the disk electrode (ω=2 πN, N is the rotation speeds), n is the number of electrons transferred during the ORR, F is the Faraday constant (F=96485 C mol^{-1}), C_0 is the O$_2$ concentration in the solution (for PH=7, 0.1M PBS solution, C_{O2}=1.2×10^{-3} mol L^{-1}), D is the diffusion coefficient of dissolved O$_2$ in the solution (for PH=7 0.1M PBS solution, D=1.9×10^{-5} cm^2 s^{-1}), and η is the viscosity of the solution (1.00×10^{-2} cm^2 s^{-1}) [34].

As we all know, the reduction of oxygen usually undergo in two pathways: a direct four-electron reduction pathway where O$_2$ is directly reduced to H$_2$O or a two-electron reduction pathway where O$_2$ is reduced to hydrogen peroxide (H$_2$O$_2$). Thus the electron transfer number (n) can be used to

determine catalytic mechanism of the catalyst during ORR. The four-electron pathway is apparently superior to the two-electron pathway in a fuel cell process [35]. As shown in Fig. 6c, 6d, the linearity and parallelism of K-L plots indicate the consistent electron transfer at -0.5, -0.6 and -0.7 V for both of the catalysts. According to above equations, the average n values were calculated to be 3.9 for the CuPInPhen/C catalyst, while the values are 3.7, 3.8, and 3.8 for the FePInPhen/C catalyst. It can be confirmed that CuPInPhen/C and FePInPhen/C catalysts take a four-electron predominant ORR mode and indicate a excellent electrocatalytic activities. Furthermore, the CuPInPhen/C catalyst shows the better onset ORR potential and the higher maximum current density compared with that of the FePInPhen/C composite. In this sense, the CuPInPhen/C catalyst is a more preferable electrocatalyst with excellent eletrocatalytic ORR performances between two composite catalysts.
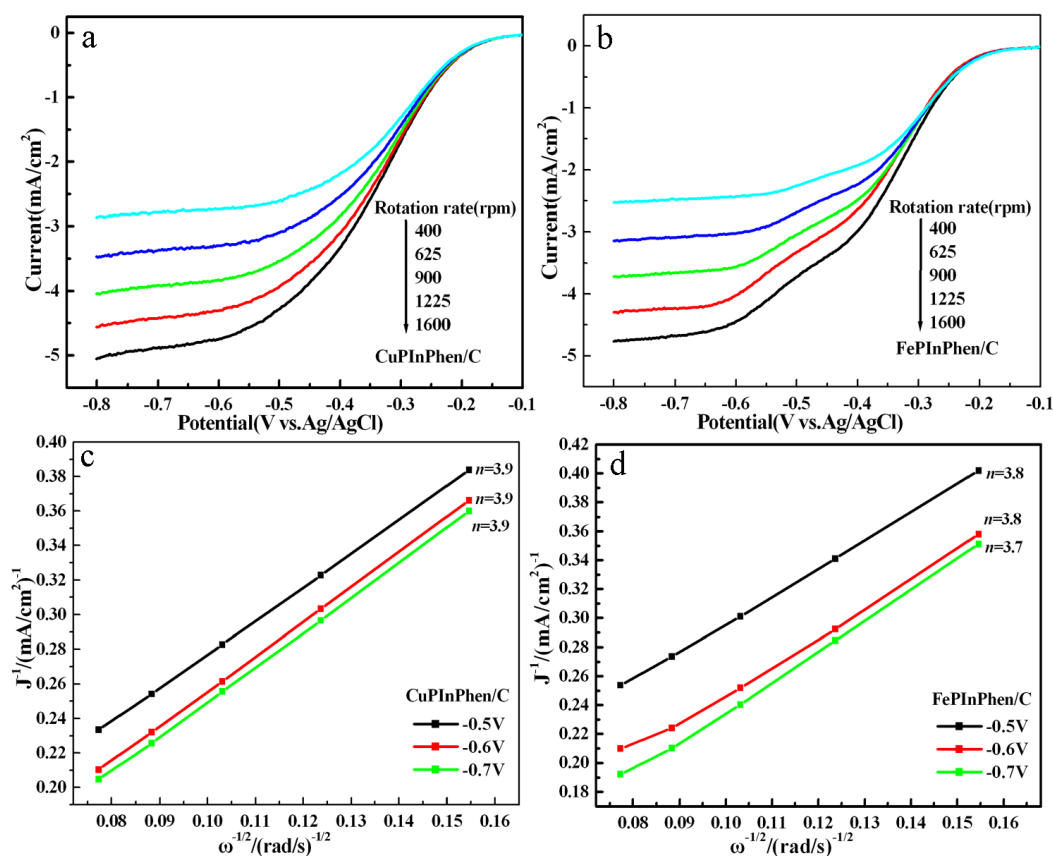

Figure 6. (a), (b) Rotating disk electrode (RDE) linear sweep voltammograms of CuPInPhen/C, FePInPhen/C with various rotation rates in O_2-saturated 0.1 M PBS at a scan rate of 10 mV s^{-1}. (c), (d) K-L plots and electron transfer numbers of CuPInPhen/C, FePInPhen/C at -0.50, -0.60 and -0.70 V.

3.2.3 RRDE measurement of the catalyst

The RRDE study was also employed to confirm the results from the RED measurement by analysising the peroxide yield during the O_2 reduction process. As shown in Fig. 7a, 7b, RRDE measurement was undertaken in O_2-saturated PBS buffer at the rotation rates of 400, 625, 900, 1225,

1600 rpm, respectively. The disk and ring currents exhibit two regions: the lower curves show curvilinear relationship between currents and voltages at the surface of disk electrode derived from the reduction of oxygen, while the upper curves show the currents arising from the oxidation of H_2O_2 by setting the electrode potential at 1.0 V. These datas obtained from RRDE can be used to calculate the electron number (n) and the formation of H_2O_2 (%) during the ORR and the equations were listed below [36]:

$$n = \frac{4i_d}{i_d + (i_r / N)} \qquad (3)$$

$$\% H_2O_2 = \frac{200i_r / N}{i_d + (i_r / N)} \qquad (4)$$

Where i_r and i_d are the ring current and disk current respectively, N is the ring collection efficiency which was determined to be a constant value of 0.37 according to the instruction book.
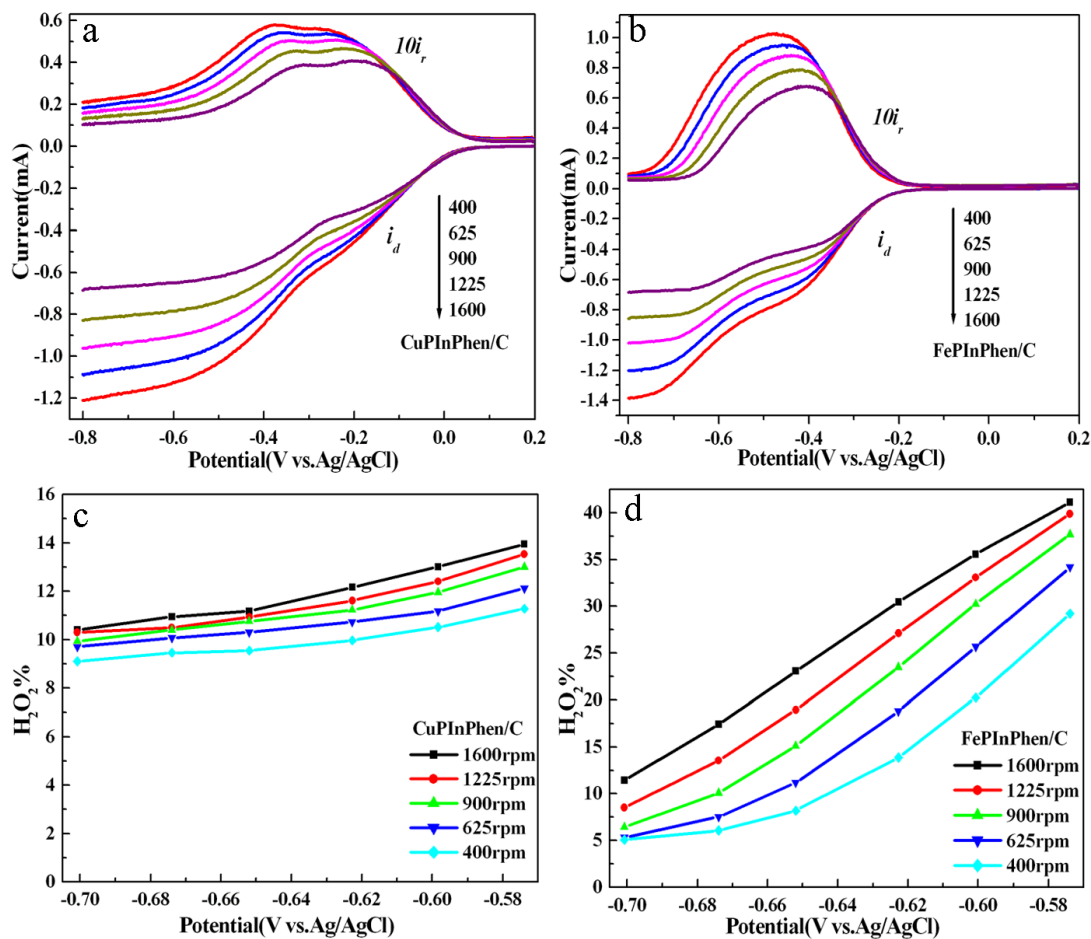

Figure 7. RRDE curves of CuPInPhen/C (a), FePInPhen/C (b) catalysts for the ORR with various rotation rates in O_2-saturated 0.1 M PBS at a scan rate of 10 mV s^{-1}, and the applied ring electrode was setted at 0.8 V. (c), (d) The %H_2O_2 production yields of the CuPInPhen/C and FePInPhen/C at various rotation rates in 0.1 M O_2-saturated PBS aqueous solutions, respectively.
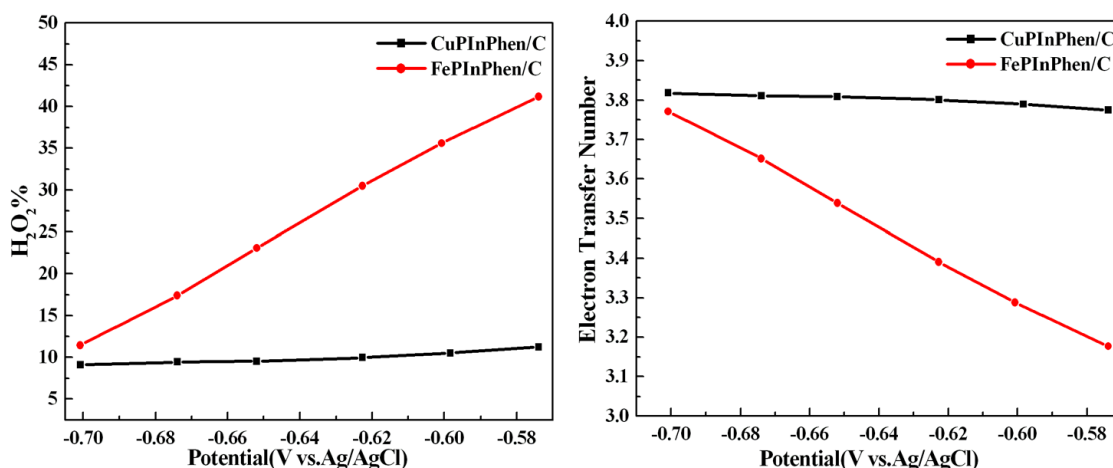
Figure 8. (a) H_2O_2 production of CuPInPhen/C and FePInPhen/C on disk potentials ranging from -0.7 to -0.58 V at 1600 rpm. (b) the corresponding electron transfer numbers calculated from RRDE curves.

As shown in Fig. 7c, 7d, the calculated H_2O_2 (%) production from the RRDE curves between -0.57 V and -0.7 V significantly dropped with the increase in rotation speeds, since high rotation speeds could result in more rapid oxygen diffusion to the electrode surface during the RRDE measurement. According to above equations, the average electron transfer numbers for CuPInPhen/C and FePInPhen/C catalysts were calculated to be 3.81 and 3.47 (Table 1), respectively. And Fig. 8 also exhibits the H_2O_2 (%) production and electron transfer numbers at a rotation rate of 1600 rpm. The CuPInPhen/C catalyst shows an average H_2O_2 production of about 9.9%, which is much lower than that of FePInPhen/C (26.5%) (Table 1). All the results above indicating that both of these two catalysts are four-electron dominantly process where O_2 is directly reduced to H_2O which is in accordance with the data from the RDE studies. However, Regarding the convectional factors at lower rotation speed (400 rpm in our study) which may interfere with the electrode measurements [37], the results from the K-L plots are likely to be more reliable.

Table 1. Comparison of electrochemical data for CuPInPhen/C and FePInPhen/C.

Modifier	E_{peak} (V vs. Ag/AgCl)	E_{onset} (V vs. Ag/AgCl)	$I_{E=-0.55\ V}$ (400 rpm) (mA/cm^2)	n @ -0.6 V (K-L)	Average n (RRDE)	Average %H_2O_2
CuPInPhen/C	-0.2483	-0.081	4.58	3.9	3.81	9.9
FePInPhen/C	-0.2995	-0.122	4.13	3.8	3.47	26.5

3.2.4 Electrochemical impedance spectra measurement of the catalyst

In this study, electrochemical impedance spectra (EIS) was used to evaluate the properties of different catalysts. Fig. 9a shows the Nyquist plots of the CuPInPhen/C and the FePInPhen/C

composite measured at open circuit potential in 0.1 M KCl solution containing 1.0 mM $K_3Fe(CN)_6$ and 1.0 mM $K_4Fe(CN)_6$ [38]. To further compared the performances of the catalysts, Nyquist plots of the CuPInPhen/C and the FePInPhen/C composite were examined at 1.0 V in the same solution. From the Fig. 9b, it can obtain a obvious semicircle from the EIS plots of samples which was usually used to measure the charge transfer resistance of the catalyst. A higher diameter of the primary semicircle leading a greater charge transfer resistance which is the mainly controlling factors to describe how fast the rate of charge transfer is during the ORR process [39].
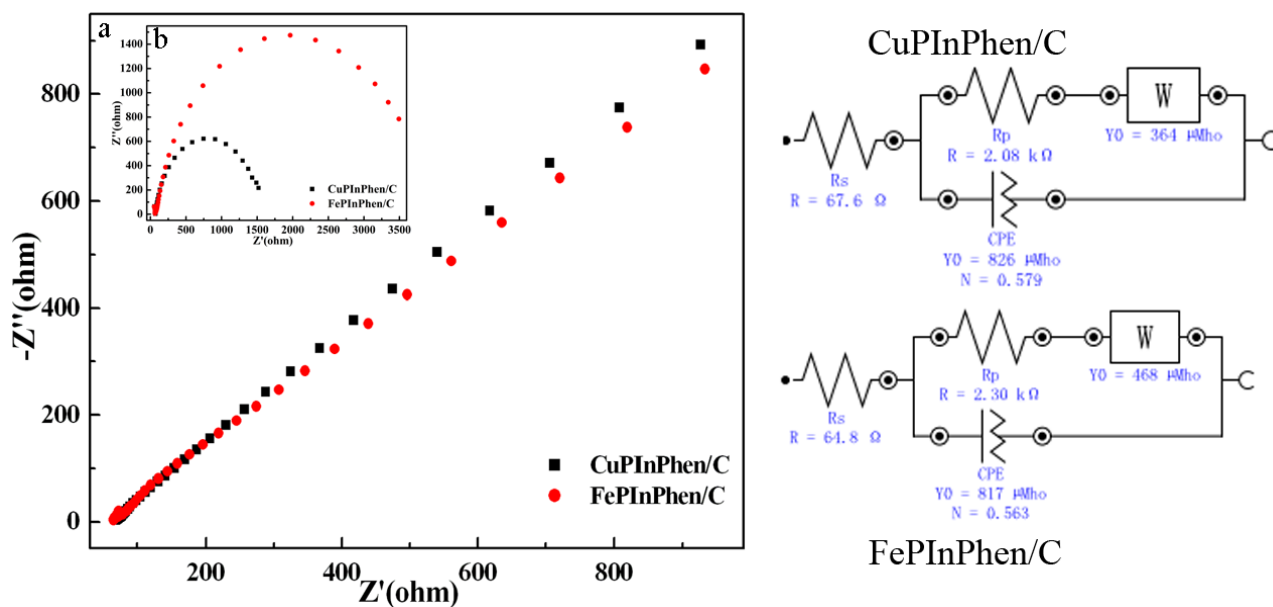

Figure 9. (a), (b) EIS plots of CuPInPhen/C and FePInPhen/C in 0.1 M PBS containing 1.0 mM $K_3Fe(CN)_6$ and 1.0 mM $K_4Fe(CN)_6$ at 0.19 V (open circuit potential), 1.0 V and the corresponding equivalent circuits.

The charge transfer resistance of the catalysts also can be compared by equivalent electric circuit as shown in the inset (right). The simple equivalent circuit including the elements R_s, R_p, *CPE* and *W* was used to fit the EIS data. Among these datas, R_p is the charge transfer resistance which usually have negative correlations with the higher electrocatalytic activities of the catalysts. We can observe from this table that the charge transfer resistance (R_p) value of CuPInPhen/C is smaller than that of FePInPhen/C, indicating CuPInPhen/C catalyst has better conductivity, and which may lead to a faster electron transfer. We can also found in equivalent electric circuit of the CuPInPhen/C and the FePInPhen/C that the values of CPE and W for the catalysts are different with each other, which might be attributable to the different metal ions complexed with the PInPhen/C matrix [40]. Moreover, the catalyst doped with copper ions (CuPInPhen/C) exhibit better electrochemical properties compared to the catalyst (FePInPhen/C) doped with ferric ion in this study. All these results above including CV data, RDE data and RRDE data aforementioned showed that the CuPInPhen/C catalyst is the better efficient electrocatalyst with good conductivity and electrocatalytic ORR activities.

Table 2. Values of elements in the equivalent circuits.

Modifier	R_s (ohm)	R_p (kohm)	CPE (µMho)	W (µMho)
CuPInPhen/C	67.6	2.08	826	364
FePInPhen/C	64.8	2.30	817	468

4. CONCLUSIONS

In summary, two hybrid composites including CuPInPhen/C and FePInPhen/C were facilely prepared by covalently bonding of the 1,10-phenanthroline metal complex to the poly(Indole-6-carboxylic acid)/C matrix. It is found that both of two catalysts can reduce oxygen by a predominant four-electron pathway and the metal cation plays a key role to enhance the electrocatalytic activity. The results of the present manuscript revealed that the new catalysts can be applied as an efficient and less expensive cathode catalysts for oxygen reduction reaction. This platinum-free but efficient organic material may be used on a large scale for practical applications in energy storage, biosensor, and electrocatalysis in future.

References

1. A. Iwan, M. Malinowski, G. Pasciak, *Renew. Sust. Energ. Rev*, 49 (2015) 954.
2. S. Bose, T. Kuila, T.X.H. Nguyen, N.H. Kim, K-T Lau, J.H. Lee, *Prog. Polym. Sci*, 36 (2011) 813.
3. T. Maiyalagan, X.C. Dong, P. Chen, X. Wang, *J. Mater. Chem*, 22 (2012) 5286.
4. E. Antolini, *Appl. Catal. B*, 181 (2016) 298.
5. D. Chen, X. Zhao, S. Chen, H.F. Li, X.N. Fu, Q.Z. Wu, S.P. Li, Y. Li, *Carbon*, 68 (2014) 755.
6. B.N. Wanjala, B. Fang, R. Loukrakpam, Y. S. Chen, M. Engelhard, J. Luo, J. Yin, L.F. Yang, S.Y. Shan, C.J. Zhong, *ACS Catal*, 2 (2012) 795.
7. M.K. Carpenter, T.E. Moylan, R.S. Kukreja, M.H. Atwan, M.M. Tessema, *J. Am. Chem. Soc*, 134 (2012) 8535.
8. C.H. Cui, H.H. Li, X.J. Liu, M.R. Gao, S.H. Yu, *ACS Catal*, 2 (2012) 916.
9. E. Antolini, R.R. Passos, E.A. Ticianelli, *Electrochim. Acta*, 48 (2002) 263.
10. C.V. Rao, A.L.M. Reddy, Y. Ishikawa, P.M. Ajayan, *Carbon*, 49 (2011) 931.
11. Y. Gorlin, C-J Chung, D. Nordlund, B.M. Clemens, T.F. Jaramillo, *ACS Catal*, 2 (2012) 2687.
12. F. Jaouen, E. Proietti, M. Lefèvre, R. Chenitz, J-P Dodelet, G. Wu, H.T. Chung, C.M. Johnston, P. Zelenay, *Energy Environ. Sci*, 4 (2011) 114.

13. H. Cheng, X.L. Feng, D.L. Wang, M. Xu, K. Pandiselvi, J.Y. Wang, Z.J. Zou, T. Li, *Electrochim. Acta*, 180 (2015) 564.
14. M. Jaymand, M. Hatamzadeh, Y. Omidi, *Prog. Polym. Sci*, 47 (2015) 26.
15. X.L. Li, Q.N. Zhong, X.L. Zhang, T.T. Li, J.M. Huang, *Thin Solid Films*, 584 (2015) 348.
16. B.B. Berkes, A.S. Bandarenka, G.*J.* Inzelt, *Phys. Chem. C*, 119 (2015) 1996.
17. W. Xia, J. Masa, M. Bron, W. Schuhmann, M. Muhler, *Electrochem. Commun*, 13 (2011) 593.
18. K. Lota, G. Lota, A. Sierczynska, I. Acznik, *Synth. Met*, 203 (2015) 44.
19. M. Zhang, W. Yuan, B. Yao, C. Li, G. Shi, *ACS Appl. Mater. Interfaces*, 6 (2014) 3587.
20. M.A. Thorseth, C.E. Tornow, E.C.M. Tse, A.A. Gewirth, *Coordin. Chem. Rev*, 257 (2013) 130.
21. Y. Lei, F.C. Anson, *Inorg. Chem*, 33 (1994) 5003.
22. C.C.L. McCrory, A. Devadoss, X. Ottenwaelder, R.D. Lowe, T.D.P. Stack, C.E.D. Chidsey, *J. Am. Chem. Soc*, 133 (2011) 3696.
23. J.F. Yu, Y.Q. Lu, C.G. Yuan, J.S. Zhao, M. Wang, R.M. Liu, *Electrochim. Acta*, 143 (2014) 1.
24. Q.F. Zhang, Y.H. Liu, X.P. Yang, Y. Hui, *Sci. China, Chem*, 57 (2013) 739.
25. A. Jaramillo, L.D. Spurlock, V. Young, A. Brajter-Toth, *Analyst*, 124 (1999) 1215.
26. A. Benkaddour, C. Journoux-Lapp, K. Jradi, S. Robert, C.*J.* Daneault, *Mater. Sci*, 49 (2014) 2832.
27. Y.Y. Shao, J.H. Sui, G.P. Yin, Y.Z. Gao, *Appl. Catal. B*, 79 (2008) 89.
28. R.Z.Yang, J.R. Dahn, A. Bonakdarpour, E.B. Easton, *J. Electrochem. Soc*, 3 (2006) 221.
29. B. Eren, L. Lichtenstein, C.H. Wu, H. Bluhm, G.A. Somorja, M. Salmeron, *J. Phys. Chem. C*, 119 (2015) 14669.
30. T. Yamashita, P. Haye, *Appl. Surf. Sci*, 254 (2008) 2441.
31. G. Bhargava, I. Gouzman, C. Chun, T. Ramanarayanan, S. Bernasek, *Appl. Surf. Sci*, 253 (2007) 4322.
32. F.Y. Cheng, Y. Su, J. Liang, L.T. Zhan, J. Chen, *Chem. Mater*, 22 (2010) 898.
33. Z. Chen, D. Higgins, Z.W. Chen, *Carbon*, 48 (2010) 3057.
34. G. Jürmann, D.J. Schiffrin, K. Tammeveski, *Electrochim. Acta*, 53 (2007) 390.
35. M. Favaro, L. Ferrighi, G. Fazio, L. Colazzo, C.D. Valentin, C. Durante, F. Sedona, A. Gennaro, S. Agnoli, G. Granozzi, *ACS Catal*, 5 (2015) 129.
36. A. Wang, A. Bonakdarpour, D.P. Wilkinson, E. Gyenge, *Electrochim. Acta*, 66 (2012) 222.
37. S.Valarselvan, P. Manisankar, *Electrochim. Acta*, 56 (2011) 6945.
38. M. Mazloum-Ardakani, A. Dehghani-Firouzabadi, M.A. Sheikh-Mohseni, A. Benvidi, B.F. Mirjalili, R. Zare, *Measurement*, 62 (2015) 88.
39. 39. S. Klink, E. Madej, E. Ventosa, A. Lindner, W. Schuhmann, F.L. Mantia, *Electrochem. Commun*, 22 (2012) 120.
40. H. Li, D. Dzombak, R. Vidic, *Ind. Eng. Chem. Res*, 51 (2012) 2821.